

Research Article

Oxidation of Enrofloxacin with Permanganate: Kinetics, Multivariate Effects, Identification of Oxidation Products, and Determination of Residual Antibacterial Activity

Yongpeng Xu,¹ Shiyao Liu,¹ Fang Guo,² and Fuyi Cui¹

¹State Key Laboratory of Urban Water Resource and Environment, School of Municipal and Environmental Engineering, Harbin Institute of Technology, Harbin 150090, China

²Academy of Fundamental and Interdisciplinary Science, Harbin Institute of Technology, Harbin 150080, China

Correspondence should be addressed to Yongpeng Xu; xuyongpeng@hit.edu.cn

Received 12 December 2014; Accepted 5 January 2015

Academic Editor: Jian Lu

Copyright © 2015 Yongpeng Xu et al. This is an open access article distributed under the Creative Commons Attribution License, which permits unrestricted use, distribution, and reproduction in any medium, provided the original work is properly cited.

Permanganate [Mn(VII)] chemistry oxidation of fluoroquinolone (FQ) antibiotic enrofloxacin (ENR) in water is investigated with respect to the kinetics, pH effect, buffer effect, and the evaluation of residual antibacterial activity after oxidative treatment. The degradation of ENR by Mn(VII) obeyed a secondary-order kinetics. Modern high-resolution tandem mass spectrometry coupled with high performance liquid chromatography was used to analyze the structures of degradation products. Four main oxidation products were identified at different pH values. Several influencing factors, pH value, and buffer obviously affect reaction rate and products relative abundance. Autocatalysis taking place at slightly acidic pH promotes the reaction but has no effect on the product types. A plausible oxidation pathway for enrofloxacin with Mn(VII) was proposed. The oxidation took place at the piperazine ring. Structural changes to the piperazine ring include N-dealkylation, hydroxylation, and hydrolysis. Residual antibacterial activity of the oxidative reaction solutions against nonresistant *Escherichia coli* reference strain DH5 α is evaluated by means of quantitative bioassays. It is noticed that the oxidation products exhibited negligible antibacterial activity just when the structures of the products changed.

1. Introduction

Enrofloxacin (ENR), a broad spectrum antibacterial agent from the class of the fluoroquinolone (FQs), is primarily and widely used in the fields of aquaculture, livestock husbandry, and human prescription [1]. Due to the incomplete metabolic transformation in mammal, ENR residual is excreted into sewerage in its pharmacokinetic forms [2–4]. Conventional water and wastewater treatment practices are inadequate for reducing antibiotic concentrations [5], leading to a continuous input into the aquatic environment. In China, FQs have been detected in surface water at concentrations ranging from 10 ng/L to 300 ng/L, and the highest concentration level of ENR was measured at 210 ng/L [6]. Along with the booming applications of ENR come potential risks to ecosystem balance [7], especially the emergence of antibiotic-resistant bacteria, so it is of great importance to investigate

the transformation of ENR in the aqueous environment [8]. A continuous input of low concentrations in WWTPs provides suitable conditions for the selective pressure toward resistant organisms [9, 10]. In addition, it was reported that more than 70% of bacteria had become sensitive against at least one antibiotic and exhibited multiple resistance patterns [11]. This may pose serious threats to the ecosystem and human health [12]. Next to resistance formation, the possible toxic effects provoked on fauna and flora are of increased concern [13, 14]. Thus, FQs are considered ubiquitous contaminants of emerging importance [15]. New treatment processes need to be developed to treat contaminated water sources and to eliminate biological activities of antibacterial compounds.

As a green and inexpensive oxidant, Mn(VII) has been widely used in water treatment for enhancing coagulation and controlling cyanotoxins and micropollutants [16–18]. In particular, Mn(VII) has been recently demonstrated to be

fairly effective in treating several FQs, ciprofloxacin (CIP), difloxacin, lomefloxacin, norfloxacin, and ofloxacin [19, 20]. Although Mn(VII) reactivity with the antibiotics was lower than that reported for ozone and free chlorine, its high selectivity and stability suggests a promising oxidant for treating sensitive micropollutants in organic-rich matrices [21].

The oxidation kinetics of ENR with Mn(VII) was investigated, and several influencing factors, solution pH value, and buffer were considered. The reaction kinetics which is highly pH-dependent can be well described by a second-order kinetic model incorporating speciation of FQs [22]. Van Doorslaer et al. [23] found that no pH dependency was noticed in the main type of moxifloxacin (MOX) degradation products formed by heterogeneous photocatalysis; a general pathway was proposed for all pH levels in this study. Autocatalysis can take place in situ forming manganese dioxides during the Mn(VII) oxidation process [24]. Solution pH and buffer can significantly affect the reaction rate. Because the autocatalysis at slightly acidic pH can promote the reaction rate, the presence of some ligands in the buffer solutions may inhibit the reaction rate.

The reaction was initiated by adding 500 μM Mn(VII) into solutions containing 10 μM ENR and a certain concentration of buffer. The process was controlled by measuring the residual ENR concentration. The reaction order was determined by the slope of $\ln([\text{ENR}]/[\text{ENR}]_0)$ versus the time plot. The loss of ENR followed the pseudo-first-order kinetics, when the Mn(VII) concentration was in large excess of the initial ENR concentration, indicating that reactions were first-order with respect to ENR. The pseudo-first-order rate constants (k_{obs} , s^{-1}) determined at Mn(VII) initial concentration of 500 μM , 21°C, neutral pH followed a second-order rate law:

$$\frac{d[\text{ENR}]}{dt} = -k_{\text{obs}} \cdot [\text{ENR}] = -k_{\text{app}} \cdot [\text{ENR}] [\text{Mn(VII)}], \quad (1)$$

where $[\text{Mn(VII)}]$ and $[\text{ENR}]$ represent the total concentrations of Mn(VII) and ENR, respectively, and k_{app} is the apparent second order rate constant for the overall reaction ($\text{M}^{-1}\text{s}^{-1}$).

The k_{app} value for the reaction (1) was determined as $0.63 \pm 0.3 \text{ M}^{-1} \text{ s}^{-1}$, which showed no significant difference from the $0.61 \pm 0.2 \text{ M}^{-1} \text{ s}^{-1}$ between Mn(VII) and CIP (a secondary amine) at neutral pH and room temperature conditions, as reported by Hu et al. [21].

With the increasing of Mn(VII) concentration, the measured k_{obs} values increased linearly. The result of the slope of pseudo-first-order rate constant k_{obs} versus Mn(VII) initial concentration plot demonstrated that the reactions were also first-order with respect to Mn(VII). From the essentiality of the reaction, increasing Mn(VII) concentration is actually increasing the oxidant molecular numbers per unit volume, leading to the increasing effective collision probability of the target compound and the oxidant molecules, and then achieving the purpose of quickly removing the target compound and improving the reaction rate.

Previous studies showed oxidation rate constant for ENR with Mn(VII) being lower than those reported for reactions with chlorine ($5.1 \times 10^2 \text{ M}^{-1} \text{ s}^{-1}$), chlorine dioxide

($62.7 \text{ M}^{-1} \text{ s}^{-1}$), and ozone ($1.5 \times 10^4 \text{ M}^{-1} \text{ s}^{-1}$) under comparable conditions, but higher than that with manganese oxide ($3.08 \times 10^{-4} \text{ M}^{-1} \text{ s}^{-1}$) [22, 25–27]. Although Mn(VII) is less reactive with ENR than chlorine, chlorine dioxide, and ozone, its attractive characteristic of high stability, relatively low cost, and nonhalogenated property is more in line with the actual production.

Furthermore, pH value has an effect on the time profiles of the reaction products; the product peak areas could be significantly influenced by solution pH value. Linke et al. [28] found that freshwater and seawater constituents, namely, humic acids (HA), Fe(III), NO_3^- , and HA- Cl^- interaction, inhibited FQs photodegradation, as they mainly acted as radiation filters and/or scavengers for reactive oxygen species. These studies shed some light on potential effect of oxidant dosage, pH value, temperature, and matrix in natural water on reaction rate constant of degradation processes. However, pH effect on Mn(VII)-ENR reaction rate has not been reported. Moreover, little information is known on the effects of reaction conditions on ENR oxidation product types and relative abundance. Studies address the Mn(VII) concentration, solution pH, and buffer effect on ENR oxidation product types and relative abundance is thus urgently required.

To date, the mechanism of oxidation by Mn(VII) is not clear and it is necessary to exclusive residual antibacterial activity of oxidation products. To evaluate the efficiency of oxidation treatment with Mn(VII), not only kinetics and process parameters are of interest, it is equally important to study the formed degradation products and residual antibacterial activity after oxidation treatment [20, 29]. Although FQs could be decomposed by chemical oxidants and photolysis; recent studies revealed that FQs were transformed without complete mineralization. To evaluate the overall efficacy of these oxidants, it is most important to study the residual antibacterial activity of oxidation products.

In this work, the reactions of the important anthropogenic contaminant ENR with aqueous Mn(VII) were studied. Detailed kinetics experiments were conducted to characterize reactions, including examining the effects of solution pH value and buffers in solutions on kinetics of Mn(VII)-ENR reactions. The main oxidation products were identified and products abundance in different reaction conditions was also compared to illuminate the effect of Mn(VII) oxidation in different conditions. Lastly, the residual antibacterial activity of the reaction solutions with neutral pH for a representative species of bacteria was examined. And the relationship between products structures and antibacterial activity was analyzed.

2. Materials and Methods

2.1. Reagents and Materials. Enrofloxacin was provided by Sigma-Aldrich with >98% purity, and all other reagents employed were of reagent grade or higher in quality. Stock of ENR was prepared in methanol/ H_2O mixture (50/50 v/v) at 1 mM and stored in a 4°C freezer protected from light for a maximum of one month. Stock of sodium thiosulfate (50 mM) as a scavenger of oxidants was prepared by dissolving a certain quantity of $\text{Na}_2\text{S}_2\text{O}_3$ crystals in deionized water.

Buffers were used to control pH for consistency and renewed weekly. The required concentrations of Mn(VII) solutions were prepared by diluting stock solution with deionized water. For the antibacterial activity bioassays Luria-Bertani (LB) broth and solid mediums were used. The antibacterial activities of the samples were determined against nonresistant *Escherichia coli* (*E. coli*) reference strain DH5 α .

2.2. Batch Experiments. Batch reactors were used to measure the reaction kinetics of ENR with Mn(VII). Experiments were conducted in 40 mL screw-cap amber borosilicate glass bottles with Teflon septa, under constant stirring on a magnetic stir plate at 21°C (in triplicate). Temperature was controlled by a thermostatic water bath. Reaction solutions were maintained at constant pH with 20 mM buffer (acetate buffer for pH 4-5, phosphate buffer for pH 6-8, and borate buffer for pH 9-10). The pH difference between initial and final samples was less than 0.1. Reactions were initiated by adding 500 μ M Mn(VII) stock solution into the solution containing a certain concentration of ENR (10 μ M for kinetics experiment and 250 μ M for observation of pH effect on product types and distributions) and 20 mM of buffer. Sample aliquots were collected periodically and immediately quenched by adding 0.1 mL of 0.2 M sodium thiosulfate, then filtered by 0.22 μ m synthetic fabric membrane, and analyzed by HPLC to determine residual ENR concentrations.

2.3. Buffer Effect Experiments. Buffer effect experiments were adapted from procedures described at the batch experiments, only with higher ENR concentrations (250 μ M) and different buffers (barbituric acid, citric acid, sodium phosphate, potassium phosphate, and sodium pyrophosphate) to measure solution pH value at 7.0.

2.4. Products Separation Methods. An Agilent 1200 high performance liquid chromatography (HPLC) with a DAD was employed to separate the residual ENR and the oxidation products obtained from the batch experiments. A volume of 20 μ L aliquot of the sample was injected into the HPLC running on the mobile phase of 89:11 (v/v) of acidified ultrapure water (0.3% acetic acid)/acetonitrile. The separation was performed using a Zorbax Extend-C18 (4.6 \times 250 nm, 5 μ m) at the flow rate of 0.4 mL \cdot min⁻¹ and column temperature of 30°C. UV detector wavelengths were set at 280 nm. The analytes were quantified by external standard quantification procedure. The system was calibrated using standard solutions prepared in methanol at six concentration levels by serial dilutions from stock solution. The peak area versus injected amount chart was obtained as standard curve with a correlation coefficient (R_2) over 0.99.

2.5. Products Identification. Reaction mixtures at given pH were prepared by the procedures described earlier. The reactions were allowed for 24 h to reach completion and then quenched by adding 0.1 mL of 0.2 M sodium thiosulfate. The samples were filtered through 0.22 μ m glass fiber membranes before using the HPLC-HRMS/MS. The samples were stored at 4°C and used within two days. All experiments were run

in duplicate, and the data were averaged. The standard deviations were usually within 5% unless otherwise noted. Agilent Technologies liquid chromatography 1200 series coupled to tandem mass spectrometer Agilent Technologies 6520 series Accurate Mass Quadrupole Time-of-Flight (HPLC-Q-TOF) were used to determine the accurate mass of the oxidation products.

2.6. Antibacterial Activity Bioassays. Quantitative bioassays were used to determine the effect of Mn(VII) treatment on the microbial growth inhibition potential of antibiotic solutions. Agar diffusion methods were performed with nonresistant *E. coli* reference strain DH5 α to indicate the antibacterial activity variation during ENR degradation. *E. coli* is sensitive to some FQs and their degradation products [23]. The sensitivity of the selected *E. coli* reference strain to ENR was estimated by using a series of concentration of the pure substrate ENR and determined that the sensitive concentration of *E. coli* DH5 α was 0.18 μ M.

A stepwise dilution series of *E. coli* were spotted onto agar plates in triplicate and incubated on sterile LB solid medium at 30°C for 24 h. The rates of survival of cells (expressed as percentages) were calculated by dividing the number of CFU of stressed cells by the number of CFU of cells before stress exposure. CFU were measured in parallel on Mn(VII)-ENR reaction solutions (solution B), ENR standard dilution (solution C), and antibiotic-free blanks (solution A). In this way the contribution of residual ENR could be distinguished from the activity of oxidation products. All growth media were sterilized by autoclaving. No extra efforts were made to exclude buffer and oxidant reduction products because preliminary experiments showed that *E. coli* was not sensitive to these compounds.

3. Results and Discussion

3.1. Effect of pH Value on Mn(VII)-ENR Reaction Rates. Solution pH values can influence the form of the oxidant and the adsorption performance of intermediate manganese dioxide. The effect of pH on the reaction was studied at the constant Mn(VII) and ENR initial concentrations of 500 μ M and 10 μ M, respectively. And the temperature of the solutions remained 21°C. The pH values ranged from 4.0 to 10.0. Figure 1(a) shows the effects of solution pH on apparent second-order rate constant of Mn(VII) reaction with ENR. As can be seen, the pH of the solution exerted a clear influence on the reaction rate of ENR. The magnitudes of k_{app} decreased substantially as pH increased from 4.0 to 5.0, but weakly increased as pH continued increasing to 9.0 and then weakly decreased as pH increased to 10.0. The fitting curves depicted in Figure 1(a) showed that Mn(VII)-ENR reaction rates were slower under neutral and alkaline environment relative to acidic environment, and the difference between neutral and alkaline environment was not big. So acidic solution is more advantageous to Mn(VII) to remove ENR. This effect of pH is corresponding to the oxidative ability of Mn(VII). Mn(VII) has different forms in different solution pH values. The redox potential of Mn(VII) in acidic, neutral, and alkaline environment is +1.51 V, +0.588 V, and 0.564 V,

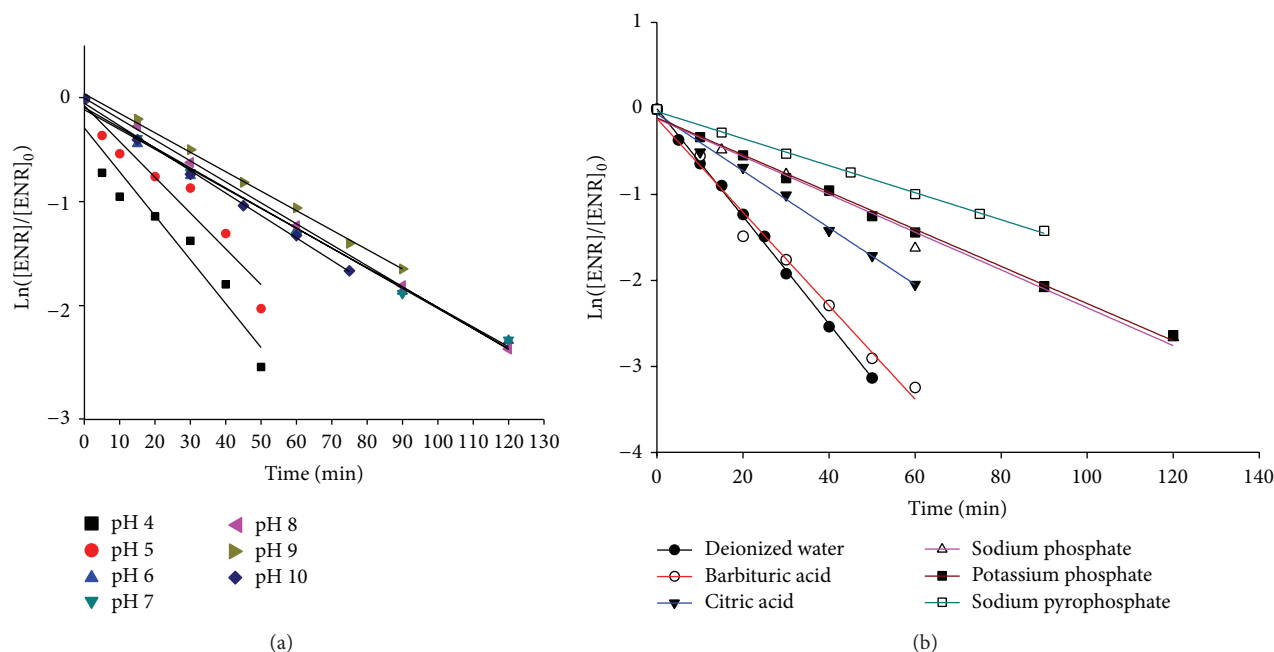


FIGURE 1: The time course of ENR ($10 \mu\text{M}$) oxidation with Mn(VII) ($500 \mu\text{M}$) at pH 4.0–10.0, acetate buffer for pH 4–5, phosphate buffer for pH 6–8, borate buffer for pH 9–10 (a); the time course of ENR ($10 \mu\text{M}$) oxidation with Mn(VII) ($500 \mu\text{M}$) in solutions with different buffers. Experimental condition: $[ENR]_0 = 10 \mu\text{M}$, $[\text{KMnO}_4]_0 = 500 \mu\text{M}$, pH 7.0, and $T = 21^\circ\text{C}$ (b).

respectively. The redox potential of Mn(VII) in acidic environment is nearly three times as much as in neutral or alkaline environment. Oxidation potential of Mn(VII) decreases with increasing pH value. This pH dependence of measured k_{app} is contrasted to the kinetics data of CIP oxidation by Mn(VII), reported by Hu et al. Thus, it may be concluded that ENR has the different oxidation process with CIP.

On the other hand, the process of Mn(VII)-ENR reaction accumulated manganese dioxide, leading to obvious autocatalysis. At solution pH 4.0 and 5.0, Mn(VII) generated manganese dioxide during the oxidation process. The surface catalyzation of manganese dioxide promoted the degradation of ENR. The mechanism of manganese dioxide catalyze Mn(VII) oxidation degradation of organic matters is similar to manganese dioxide oxidation separately [30]. Organic matters are first absorbed to the surface of manganese dioxide, forming the surface complexes. Then electron transfer between the surface complexes and Mn(VII) takes place, while, in the process of manganese oxidation separately, intramolecular electron transfer takes place between surface complexes themselves. Jiang et al. [24] employed Mn(VII) to oxidate triclosan, phenol, and 2,4-dichlorophenol, confirmed the loss of the target compounds displayed autocatalysis.

3.2. Effect of Buffers on Mn(VII)-ENR Reaction Rates. To further verify the mechanism proposed above, the effect of six buffers (i.e., barbituric acid, citric acid, sodium phosphate, potassium phosphate, and sodium pyrophosphate) on Mn(VII)-ENR reaction was studied. Figure 1(b) shows the effects of buffer on apparent second-order rate constant of Mn(VII) reaction with ENR. As can be seen, k_{app} showed a significant difference among different reaction systems.

From the above conclusion, Mn(VII)-ENR reaction followed a second-order rate law and the oxidant concentration kept constant, reaction rate constant K , and pseudo-first-order constant k_{obs} have positive correlation, thus indicated that the reaction rate constant K was affected by different buffers. The second-order rate constants of deionized water, barbituric acid, citric acid, sodium phosphate, potassium phosphate, and sodium pyrophosphate are indicated with K_q , K_b , K_n , K_{la} , K_{lk} , and K_j , respectively. By the slopes of the fitting curves in different reaction systems we can clearly see that $K_q > K_b > K_n > K_{la} \sim K_{lk} > K_j$, shows that the degree of effect on the reaction rate by buffers was increasing successively. The reaction rate of deionized water was the maximum; barbituric acids and citric acids took second place; phosphates and pyrophosphates were the least. The buffers selected in this study inhibited the reaction rate more or less. This can be explained by the change of pH value in deionized water; the initial pH value in deionized water was 7.11 and, after 30 min and 60 min, the pH values were 7.01 and 6.89, respectively, while the pH values kept constant in solutions with buffers. The presence of H^+ or OH^- in solution may affect the ratio of the target compound ions distribution, which affects the reaction rate. What is more, the results might be also ascribed to the presence of some ligands in the buffer solutions which can occupy the oxidation points (H atoms on the N4), so that they may inhibit the reaction rate.

3.3. Reaction Scheme. The experiments conducted above showed that solution pH values and buffers can clearly affect the reaction rate. To verify that if pH values and buffers can change the main reaction pathways, the oxidation product forms and relative abundance were analyzed. To determine

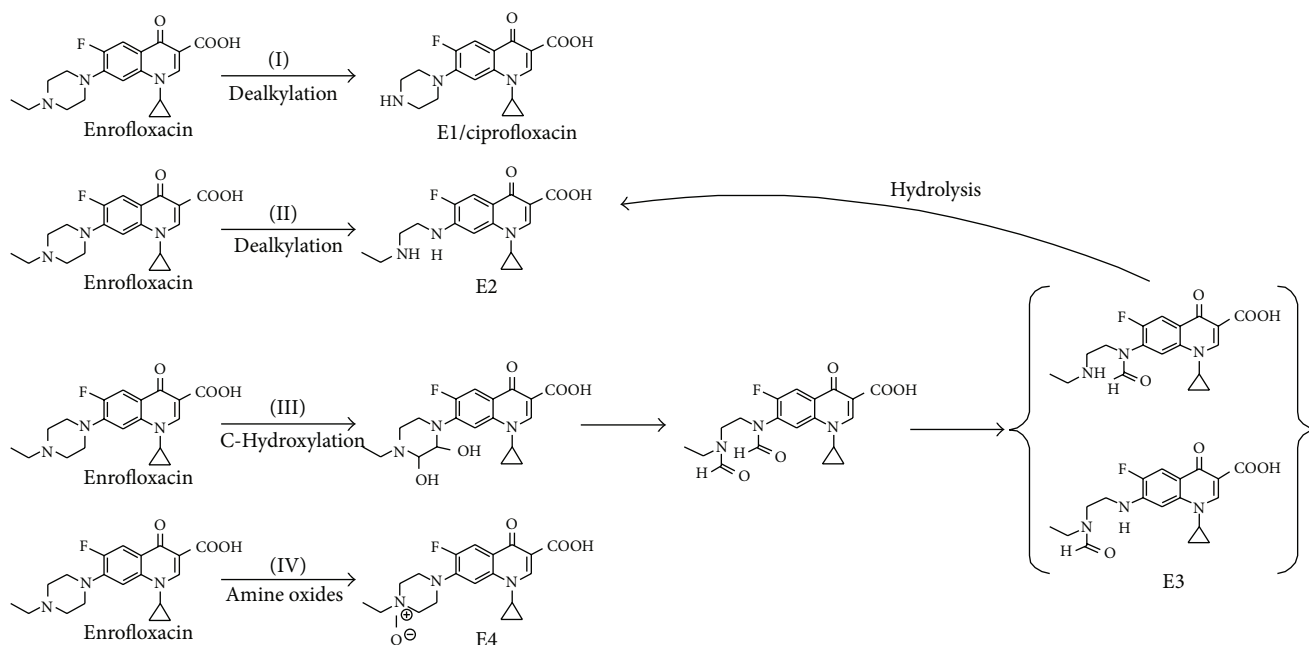


FIGURE 2: Proposed reaction pathways and products in the oxidation of ENR by Mn(VII).

the degradation products, the HPLC-MS screening of complex mixture samples were performed and followed by targeted MS/MS analysis. The accurate mass of the protonated molecular ion $[M+H]^+$ obtained from MS scan enables the molecular formula of a product. Then, structures for these products are proposed based on the molecular composition of the mother compound. Subsequently, acquired targeted MS/MS spectra data deliver confirmatory information.

Under the reaction conditions that Mn(VII) has initial concentration of $500 \mu\text{M}$, ENR initial concentration of $10 \mu\text{M}$, neutral pH and constant temperature of 21°C , and liquid chromatogram pre-separated result exhibited four significant peaks directing four dominant products transformed. With the retention time extending, the molecular ions of m/z are 362.1515 (E3), 334.1568 (E2), 332.1410 (E1/CIP), and 376.1672 (E4), sequentially. The probable structures proposed for the main products are provided in Figure 2.

When all the experiment conditions remained the same, only with the solution pH values changed, the concentration of residual ENR, the oxidation product structures, and the abundance of the oxidation products were analyzed by HPLC with a DAD. No pH dependency is noticed in the main type of oxidation products formed; the reaction pathway proposed below can be acknowledged as a general pathway for all pH levels. Nevertheless a pH effect on the abundance of products was observed in the complete reaction solutions. The relative abundance of the identified compounds in the liquid phase as a function of pH, in terms of maximum peak area observed during oxidation process, is presented in Figure 3. Among the investigated pH levels, residual ENR showed the highest occurrence at neutral conditions and the lowest occurrence at deionized water without pH adjustment, which was corresponding to the result of the kinetics experiment.

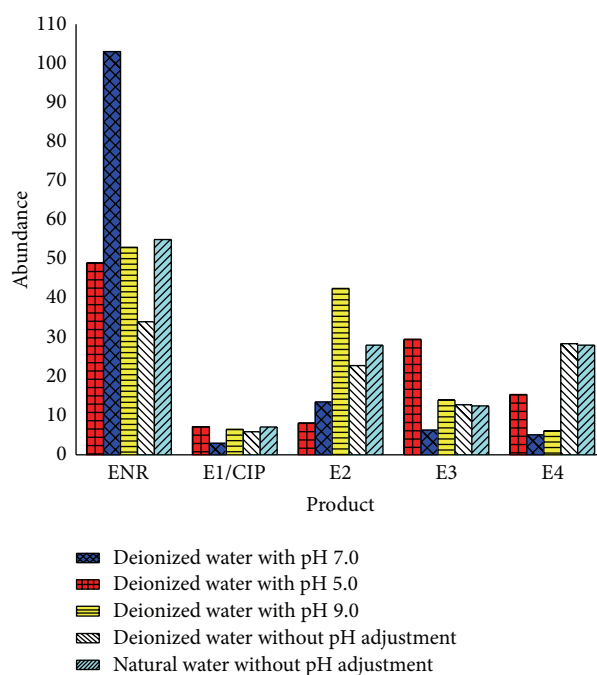


FIGURE 3: ENR oxidation products relative abundance in deionized water with pH 5.0, deionized water with pH 7.0, deionized water with pH 9.0, deionized water without pH adjustment, and natural water without pH adjustment. Experimental condition: $[\text{ENR}]_0 = 10 \mu\text{M}$, $[\text{KMnO}_4]_0 = 500 \mu\text{M}$, and $T = 21^\circ\text{C}$.

Phosphate buffer in solutions at neutral conditions might also play a part because phosphate can inhibit the reaction rate. There was little difference in terms of the evolvement trends of the four main products in deionized and natural water, but clearly different from the deionized water with pH 7.0, which

indicates that buffers can affect ENR oxidation products relative to abundance in solutions. Besides, the main products kept the same indicate that autocatalysis at slightly acidic pH just influence the reaction rate but have no effect on reaction pathway and product generation. Product E1/CIP abundance was lower at pH 7.0, while nearly flat at other pH values. Product E2 abundance was highest at alkaline condition and lowest at acidic condition, while products E3 and E4 were just the opposite. This may attribute to the product structures formed by the N-dealkylation, C-hydroxylation, and amine oxides. The ratio of E2 was always in the majority among these four main products except at pH 5.0. A possible reason for this difference could be the influence of pH on the reaction speeds in the pathway favoring specific reactions or slowing down others, creating "bottle-necks."

According to the conclusion mentioned above, general plausible reaction pathways for all pH levels were proposed. The reactions mainly occurred on the piperazine ring and the core FQ structure remains intact in all the products identified. There are three principal Mn(VII) reaction pathways in Mn(VII)-ENR reaction. As shown in Figure 2, the oxidation of the piperazine resulted in N-dealkylation (pathway I and II), C-hydroxylation (pathway III), and amine oxides (pathway IV). The initiation step of Mn(VII)-ENR reactions is proposed to be the oxidative formation of an enamine (E2) from the aromatic amine group; as reported by Rawalay and Shechter [31], E2 can then be transformed by multiple parallel reactions to produce a series of products through either hydrolysis or further Mn(VII) oxidation of the newly formed C=C double bonds [32, 33]. The partially dealkylated product E1 is formed when E2 undergoes two consecutive hydrolysis steps. Collectively, the identified reaction products indicate that Mn(VII) reactions alter the piperazine substituent but leave the core fluoroquinolone group intact, so it is unclear how oxidation by Mn(VII) will affect the antibacterial activity of ENR solutions.

3.4. Residual Antibacterial Activity. As shown above, ENR can be oxidized easily by Mn(VII), and all the products identified retain the quinolone core, which has significant relationship with antibacterial activities [34]. The degraded ENR solution (solution B) was compared with a proper dilution (solution C) of the original compound, in order to elucidate the bacterial growth inhibition potential of Mn(VII)-ENR reaction products. The antibacterial activity evolution of ENR during the oxidation was assayed at pH 7.0. Solution B and solution C have a similar antibacterial activity evolution trend; until 100 min, they all reached to the level of solution A and displayed no inhibition against *E. coli* DH5 α . The result of bioassay is shown in Table 1.

Therefore, the residual antibacterial activity of the Mn(VII)-treated solutions (solution B) is mostly correlated well with the residual amount of parent compound in solution in the case Mn(VII) excess. This indicates that the mixture degradation products oxidized by excess Mn(VII) contribute ignorable antibacterial activity against *E. coli* DH5 α comparing to the parent antibiotic. According to a widely accepted model for FQs-DNA cooperative binding in the inhibition of DNA gyrase, the quinolone core which contains a carboxyl

TABLE 1: The *E. coli* DH5 α CFU ratio between solutions B and C and solution A.

Time (min) ^a	Concentration of residual ENR (μ M)	Ratio between B and A ^b	Ratio between C and A ^c
0	10	0	0
20	8.27	0	0
40	5.7	0	0
60	3.4	0	$2.14E - 06$
80	2.16	$6.00E - 05$	0.08571
100	1.17	1	0.85714
120	0.53	0.9	1

^aThe reaction time of ENR with Mn(VII); ^bthe *E. coli* DH5 α CFU ratio between solution B and solution A; ^cthe *E. coli* DH5 α CFU ratio between solution C and solution A.

and keto group is of key importance for antibacterial activity [34], as shown in Figure 4. However, the product mixture remaining in the quinolone structure is observed leading to deactivation. This is because the piperazine substituent may have the function that can bind with the DNA topoisomerase enzymes; the modification on this moiety highly influences FQs antibacterial activity [1]. The transformation and/or degradation of the piperazine substituent can significantly diminish the antibacterial activity, in spite of the quinolone core keep intact. From the mass spectrum data, we can find that all the products, except E1/CIP, occurred during the transformation and/or degradation of the piperazine substituent, which is corresponding to Paul's conclusion.

These findings are notable because with the general reaction pathway, the main oxidation products generated at various reaction conditions are the same. So the antibacterial activity of the Mn(VII)-reacted solutions is mainly subject to the concentration of residual parent antibiotic. Considering that Mn(VII)-ENR reaction rates were faster under acidic environment under neutral or alkaline environment, there is no big difference between neutral and alkaline environment. Moreover, buffers also have inhibition on the reaction rate. So the residual ENR concentrations at other pH or without pH adjustment are far lower than at pH 7.0, so we can deem that the antibacterial activity is eliminated at various reaction conditions.

4. Conclusions

This study has demonstrated that the important anthropogenic contaminant ENR can be transformed by Mn(VII) to other like-quinolones products, and the degradation of ENR by Mn(VII) obeyed a secondary-order kinetics. Solution pH value and buffers can affect the reaction rates and the oxidation products relative abundance but have no effect on products types. The process of Mn(VII)-ENR reaction accumulated manganese dioxide, leading to obvious autocatalysis at slightly acidic pH. Mn(VII)-ENR reaction rates were faster under acidic environment than under neutral or alkaline environment. And the reaction rate was observably influenced by buffers, especially phosphate and pyrophosphate buffers. A plausible oxidation pathway for enrofloxacin

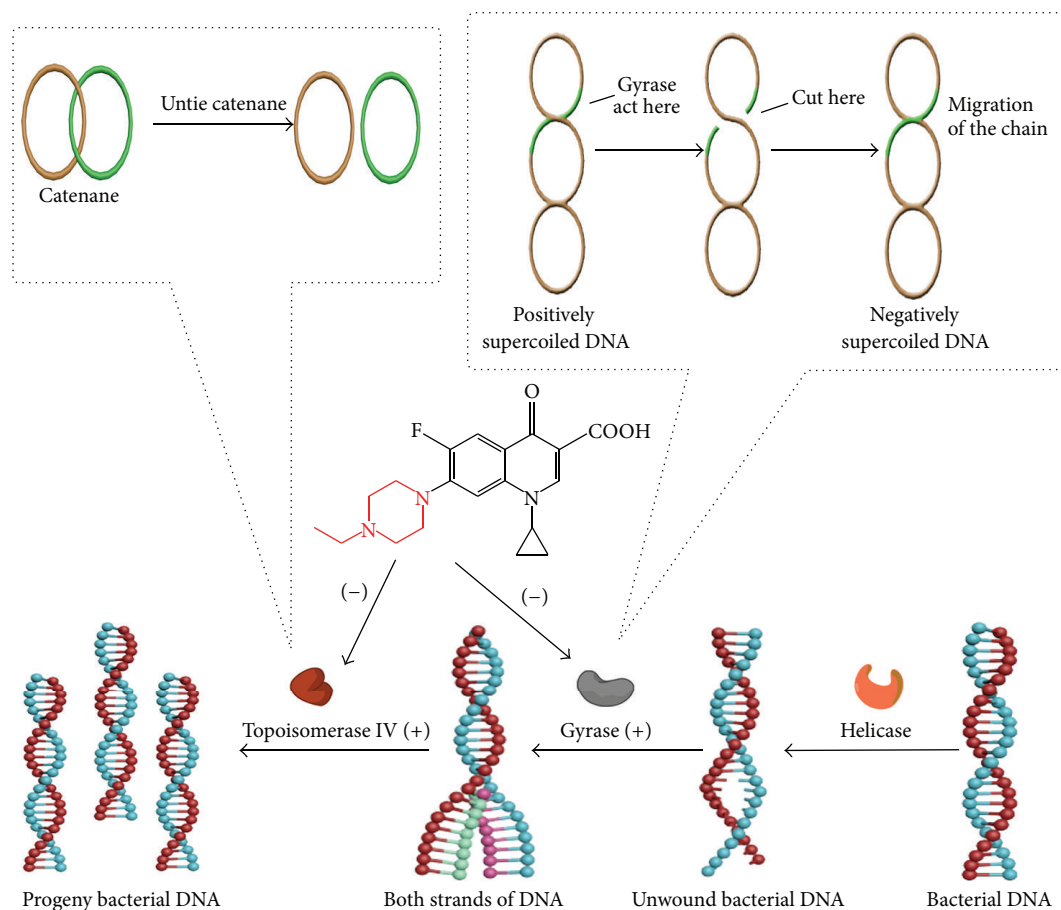


FIGURE 4: Schematic representation of mechanism of action of enrofloxacin with bacterial DNA.

with Mn(VII) was proposed. The oxidation took place at the piperazine ring. Structural changes to the piperazine ring include N-dealkylation, hydroxylation, and hydrolysis. Four main oxidation products were identified at different reaction conditions. These products expect CIP exhibit little antibacterial activity on *E. coli* DH5 α , suggesting the structures of degradation products and reactivity pathways significant correlation with antibacterial activity. So the antibacterial activity can be eliminated at various reaction conditions. These conclusions can be used to estimate antibacterial activity for many practical engineering conditions.

Conflict of Interests

The authors declare that there is no conflict of interests regarding the publication of this paper.


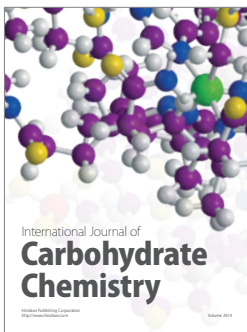
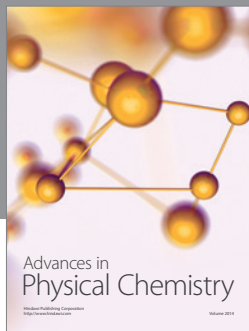
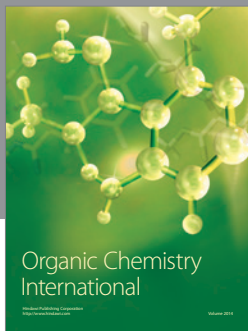
Acknowledgments

This work has been financially supported by the National Natural Science Foundation of China (51108118) and Heilongjiang Province Scholarship Foundation (LC2012C28). The authors gratefully acknowledge Dr. Yanhe Zhang (Harbin Veterinary Research Institute, CAAS) for nice help in bioassay experiment.

References

- [1] T. Paul, M. C. Dodd, and T. J. Strathmann, "Photolytic and photocatalytic decomposition of aqueous ciprofloxacin: transformation products and residual antibacterial activity," *Water Research*, vol. 44, no. 10, pp. 3121–3132, 2010.
- [2] A. Speltini, M. Sturini, F. Maraschi, and A. Profumo, "Fluoroquinolone antibiotics in environmental waters: sample preparation and determination," *Journal of Separation Science*, vol. 33, no. 8, pp. 1115–1131, 2010.
- [3] K. Kümmerer, "The presence of pharmaceuticals in the environment due to human use—present knowledge and future challenges," *Journal of Environmental Management*, vol. 90, no. 8, pp. 2354–2366, 2009.
- [4] D. Fatta-Kassinos, S. Meric, and A. Nikolaou, "Pharmaceutical residues in environmental waters and wastewater: current state of knowledge and future research," *Analytical and Bioanalytical Chemistry*, vol. 399, no. 1, pp. 251–275, 2011.
- [5] C. L. Amorim, A. S. Maia, R. B. R. Mesquita et al., "Performance of aerobic granular sludge in a sequencing batch bioreactor exposed to ofloxacin, norfloxacin and ciprofloxacin," *Water Research*, vol. 50, pp. 101–113, 2014.
- [6] R. Wei, F. Ge, M. Chen, and R. Wang, "Occurrence of ciprofloxacin, enrofloxacin, and florfenicol in animal wastewater and water resources," *Journal of Environmental Quality*, vol. 41, no. 5, pp. 1481–1486, 2012.

- [7] M. Sturini, A. Speltini, F. Maraschi et al., "Photochemical degradation of marbofloxacin and enrofloxacin in natural waters," *Environmental Science and Technology*, vol. 44, no. 12, pp. 4564–4569, 2010.
- [8] M. Lillenberg, S. Yurchenko, K. Kipper et al., "Presence of fluoroquinolones and sulfonamides in urban sewage sludge and their degradation as a result of composting," *International Journal of Environmental Science and Technology*, vol. 7, no. 2, pp. 307–312, 2010.
- [9] K. L. Jury, S. J. Khan, T. Vancov, R. M. Stuetz, and N. J. Ashbolt, "Are sewage treatment plants promoting antibiotic resistance?" *Critical Reviews in Environmental Science and Technology*, vol. 41, no. 3, pp. 243–270, 2011.
- [10] K. Kümmerer and A. Henninger, "Promoting resistance by the emission of antibiotics from hospitals and households into effluent," *Clinical Microbiology and Infection*, vol. 9, no. 12, pp. 1203–1214, 2003.
- [11] R. Hirsch, T. Ternes, K. Haberer, and K.-L. Kratz, "Occurrence of antibiotics in the aquatic environment," *Science of the Total Environment*, vol. 225, no. 1-2, pp. 109–118, 1999.
- [12] D. A. Volmer, B. Mansoori, and S. J. Locke, "Study of 4-quinolone antibiotics in biological samples by short-column liquid chromatography coupled with electrospray ionization tandem mass spectrometry," *Analytical Chemistry*, vol. 69, no. 20, pp. 4143–4155, 1997.
- [13] G. Carlsson, S. Örn, and D. G. J. Larsson, "Effluent from bulk drug production is toxic to aquatic vertebrates," *Environmental Toxicology and Chemistry*, vol. 28, no. 12, pp. 2656–2662, 2009.
- [14] I. Ebert, J. Bachmann, U. Kühnen et al., "Toxicity of the fluoroquinolone antibiotics enrofloxacin and ciprofloxacin to photoautotrophic aquatic organisms," *Environmental Toxicology and Chemistry*, vol. 30, no. 12, pp. 2786–2792, 2011.
- [15] M. Sturini, A. Speltini, F. Maraschi et al., "Sunlight-induced degradation of soil-adsorbed veterinary antimicrobials Marbofloxacin and Enrofloxacin," *Chemosphere*, vol. 86, no. 2, pp. 130–137, 2012.
- [16] J. E. van Benschoten, W. Lin, and W. R. Knocke, "Kinetic modeling of manganese(II) oxidation by chlorine dioxide and potassium permanganate," *Environmental Science and Technology*, vol. 26, no. 7, pp. 1327–1333, 1992.
- [17] E. Rodríguez, M. E. Majado, J. Meriluoto, and J. L. Acero, "Oxidation of microcystins by permanganate: reaction kinetics and implications for water treatment," *Water Research*, vol. 41, no. 1, pp. 102–110, 2007.
- [18] A. M. Dietrich, R. C. Hoehn, L. C. Dufresne, L. W. Buffin, D. M. C. Rashash, and B. C. Parker, "Oxidation of odorous and nonodorous algal metabolites by permanganate, chlorine, and chlorine dioxide," *Water Science and Technology*, vol. 31, no. 11, pp. 223–228, 1995.
- [19] U. Hubicka, P. Zmudzki, B. Zuromska-Witek, P. Zajdel, M. Pawłowski, and J. Krzek, "Separation and characterization of ciprofloxacin, difloxacin, lomefloxacin, norfloxacin, and ofloxacin oxidation products under potassium permanganate treatment in acidic medium by UPLC-MS/MS," *Talanta*, vol. 109, pp. 91–100, 2013.
- [20] L. Hu, A. M. Stemig, K. H. Wammer, and T. J. Strathmann, "Oxidation of antibiotics during water treatment with potassium permanganate: reaction pathways and deactivation," *Environmental Science and Technology*, vol. 45, no. 8, pp. 3635–3642, 2011.
- [21] L. Hu, H. M. Martin, and T. J. Strathmann, "Oxidation kinetics of antibiotics during water treatment with potassium permanganate," *Environmental Science & Technology*, vol. 44, no. 16, pp. 6416–6422, 2010.
- [22] P. Wang, Y.-L. He, and C.-H. Huang, "Oxidation of fluoroquinolone antibiotics and structurally related amines by chlorine dioxide: reaction kinetics, product and pathway evaluation," *Water Research*, vol. 44, no. 20, pp. 5989–5998, 2010.
- [23] X. Van Doorslaer, K. Demeestere, P. M. Heynderickx et al., "Heterogeneous photocatalysis of moxifloxacin: identification of degradation products and determination of residual antibacterial activity," *Applied Catalysis B: Environmental*, vol. 138–139, pp. 333–341, 2013.
- [24] J. Jiang, S.-Y. Pang, and J. Ma, "Oxidation of triclosan by permanganate (Mn(VII)): importance of ligands and in situ formed manganese oxides," *Environmental Science and Technology*, vol. 43, no. 21, pp. 8326–8331, 2009.
- [25] M. C. Dodd, A. D. Shah, U. von Gunten, and C. H. Huang, "Interactions of fluoroquinolone antibacterial agents with aqueous chlorine: reaction kinetics, mechanisms, and transformation pathways," *Environmental Science and Technology*, vol. 39, no. 18, pp. 7065–7076, 2005.
- [26] M. C. Dodd, M.-O. Buffle, and U. Von Gunten, "Oxidation of antibacterial molecules by aqueous ozone: moiety-specific reaction kinetics and application to ozone-based wastewater treatment," *Environmental Science & Technology*, vol. 40, no. 6, pp. 1969–1977, 2006.
- [27] H. Zhang and C.-H. Huang, "Oxidative transformation of fluoroquinolone antibacterial agents and structurally related amines by manganese oxide," *Environmental Science & Technology*, vol. 39, no. 12, pp. 4474–4483, 2005.
- [28] G. E. Linke, J. Chen, W. Xiaoxuan et al., "Aquatic photochemistry of fluoroquinolone antibiotics: kinetics, pathways, and multivariate effects of main water constituents," *Environmental Science & Technology*, vol. 44, no. 7, pp. 2400–2405, 2010.
- [29] X. van Doorslaer, P. M. Heynderickx, K. Demeestere, K. Debevere, H. van Langenhove, and J. Dewulf, "TiO₂ mediated heterogeneous photocatalytic degradation of moxifloxacin: operational variables and scavenger study," *Applied Catalysis B: Environmental*, vol. 111–112, pp. 150–156, 2012.
- [30] H. Zhang and C.-H. Huang, "Oxidative transformation of triclosan and chlorophene by manganese oxides," *Environmental Science and Technology*, vol. 37, no. 11, pp. 2421–2430, 2003.
- [31] S. S. Rawalay and H. Shechter, "Oxidation of primary, secondary, and tertiary amines with neutral permanganate. Simple method for degrading amines to aldehydes and ketones," *Journal of Organic Chemistry*, vol. 32, no. 10, pp. 3129–3131, 1967.
- [32] L. Hu, H. M. Martin, O. Arce-Bulted, M. N. Sugihara, K. A. Keating, and T. J. Strathmann, "Oxidation of carbamazepine by Mn(VII) and Fe(VI): reaction kinetics and mechanism," *Environmental Science and Technology*, vol. 43, no. 2, pp. 509–515, 2009.
- [33] Y. E. Yan and F. W. Schwartz, "Kinetics and mechanisms for TCE oxidation by permanganate," *Environmental Science and Technology*, vol. 34, no. 12, pp. 2535–2541, 2000.
- [34] L. L. Shen, L. A. Mitscher, P. N. Sharma et al., "Mechanism of inhibition of DNA gyrase by quinolone antibacterials: a cooperative drug-DNA binding model," *Biochemistry*, vol. 28, no. 9, pp. 3886–3894, 1989.



Hindawi

Submit your manuscripts at
<http://www.hindawi.com>

